

1

Supplementary Material

2 **Ru supported on activated carbon and coated with polydopamine**

3 **layer for effective acetylene hydrochlorination**

4 Miaomiao Zhang^a, Haiyang Zhang^{a,*}, Feng Li^a, Lisha Yao^a, Wencai Peng^{a,*}, Jinli
5 Zhang^{a,b}

6 ^aSchool of Chemistry and Chemical Engineering/Key Laboratory for Green

7 Processing of Chemical Engineering of Xinjiang Bingtuan, Shihezi University,

8 Shihezi 832000 (P.R. China); E-mail: zhy198722@163.com (H.Y. Zhang),

9 pengwencai@shzu.edu.cn. (W.C. Peng).

10 ^bSchool of Chemical Engineering and Technology, Tianjin University, Tianjin

11 300072 (P.R. China); E-mail: zhangjinli@tju.edu.cn (J.L. Zhang)

12 *Corresponding authors: Tel: +86-993-2057-277;

13 E-mail: zhy198722@163.com (Haiyang Zhang); pengwencai@shzu.edu.cn (Wencai

14 Peng)

15

1 Table and Figure captions

- 2 **Table S1** The relative content and binding energy of Ru species in the unreacted and reacted Ru-based catalysts.
- 3
- 4 **Table S2** EXAFS fitting parameters at the edge for various samples.
- 5
- 6 **Fig. S1** The (a) C₂H₂ conversion and (b) selectivity to VCM of different catalysts. Reaction condition: T=180 °C, GHSV(C₂H₂) = 180 h⁻¹, and V(HCl)/V(C₂H₂) = 1.15.
- 7
- 8 **Fig. S2** (a) Raman spectra and (b) FT-IR spectra of PDA-T materials.
- 9 **Fig. S3** FT-IR spectra of unreacted catalysts.
- 10 **Fig. S4** HAADF-STEM images of the all catalysts.
- 11 **Fig. S5** SEM images of the unreacted PDA catalysts.
- 12 **Fig. S6** HADDF-TEM images of the (a) unreacted Ru/AC@PDA-100, (b) reacted Ru/AC@PDA-100, (c) unreacted Ru/AC@PDA-500, (d) reacted Ru/AC@PDA-500, (e) unreacted Ru/AC@PDA-800, and (f) reacted Ru/AC@PDA-800.
- 13
- 14
- 15 **Fig. S7** Nitrogen adsorption-desorption isotherms of the (a) unreacted and (b) reacted catalysts.
- 16 **Fig. S8** TG curves of the unreacted and reacted catalysts recorded under air atmosphere.
- 17 **Fig. S9** MS spectra (m/z = 16) of the unreacted Ru catalysts.
- 18 **Fig. S10** Ru 3p XPS spectra of the reacted Ru catalysts.
- 19 **Fig. S11** The real/imaginary component of the FT with the scattering paths used in the fitting models.
- 20
- 21 **Fig. S12** Wavelet transform spectra of the Ru-based catalysts.
- 22 **Fig. S13** (a) N 1s XPS spectrum of the unreacted AC@PDA catalyst and (b) possible structure of PDA.
- 23
- 24 **Fig. S14** The most stable calculation model of the complex.
- 25 **Fig. S15** Energy profiles of Ru/AC catalyst for acetylene hydrochlorination.

Table S1 The relative content and binding energy of Ru species in the unreacted and reacted Ru-based catalysts.

Catalyst	Binding energy (eV) , (Area%)					
	Ru ⁿ⁺ (n>4)	Ru ⁴⁺	Ru ³⁺	Ru ^{z+} (1<z<3)	Ru ⁰	Ru ^{m+} (m≥3)
Unreacted Ru/AC	467.6 (14.2)	465.0 (17.2)	463.1 (35.0)	/	461.3 (33.6)	66.4
Reacted Ru/AC	467.3 (8.9)	464.9 (26.2)	463.1 (29.9)	/	461.5 (35.0)	65.0
Unreacted Ru/AC@PDA-100	467.3 (15.4)	465.2 (23.0)	463.9 (30.3)	462.0 (31.3)	/	68.7
Reacted Ru/AC@PDA-100	467.7 (11.1)	465.2 (18.3)	463.2 (35.7)	/	461.2 (34.9)	65.1
Unreacted Ru/AC@PDA-500	467.5 (19.7)	465.4 (22.8)	463.5 (29.6)	461.6 (27.9)	/	72.1
Reacted Ru/AC@PDA-500	467.8 (18.1)	465.1 (16.1)	463.1 (33.1)	/	461.4 (32.7)	67.3
Unreacted Ru/AC@PDA-800	467.6 (26.9)	465.7 (22.0)	463.6 (25.2)	461.6 (25.9)	/	74.1
Reacted Ru/AC@PDA-800	468.0 (12.2)	465.4 (14.6)	463.4 (33.6)	/	461.4 (39.6)	60.4

1

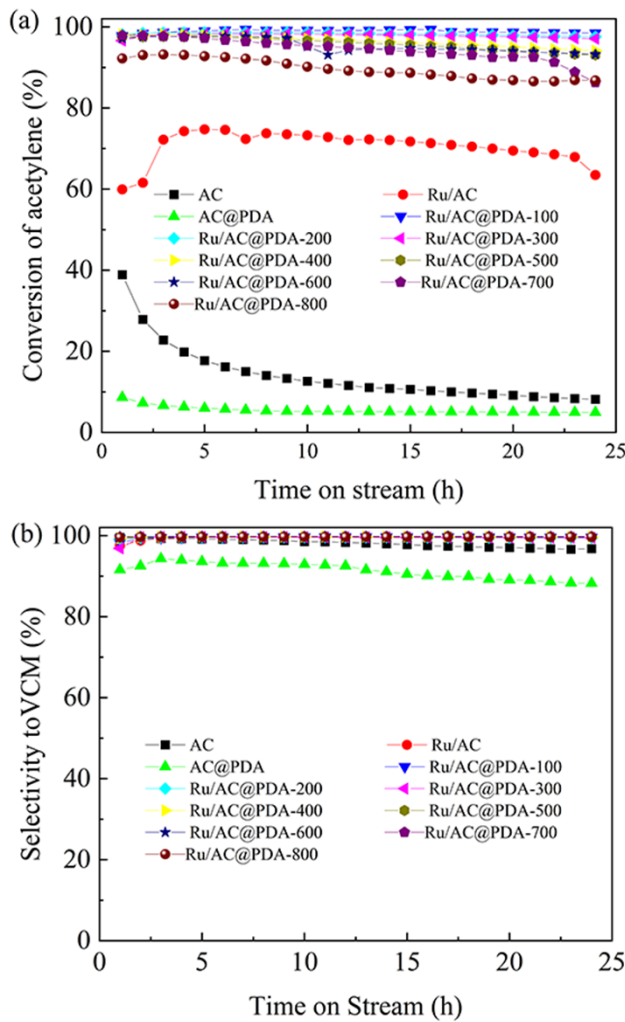
Table S2 EXAFS fitting parameters at the edge for various samples.

Sample	shell	CN	R(Å)	σ^2	ΔE_0	R factor
Ru foil	Ru-Ru	12	2.67 ± 0.01	0.0037	2.2 ± 0.7	0.0085
RuO ₂	Ru-O	7.8 ± 1.0	1.98 ± 0.01	0.0029	2.5 ± 1.9	0.0197
RuCl ₃	Ru-Cl	5.3 ± 0.5	2.35 ± 0.02	0.0036	0.2 ± 2.1	0.0227
	Ru-O/N	1.7 ± 0.4	1.81 ± 0.02	0.0021		
Ru/AC	Ru-Cl	4.2 ± 0.3	2.36 ± 0.01	0.0016	-2.0 ± 1.8	0.0139
	Ru-Ru	4.1 ± 0.6	2.60 ± 0.02	0.0071		
Ru/AC@PDA-100	Ru-O/N	5.4 ± 0.1	2.07 ± 0.01	0.0041	4.3 ± 0.7	0.0030
	Ru-Ru	1.5 ± 0.1	2.71 ± 0.01	0.0048		
Ru/AC@PDA-500	Ru-O/N	5.9 ± 0.4	2.07 ± 0.01	0.0064	2.8 ± 1.8	0.0137
	Ru-Ru	1.1 ± 0.2	2.70 ± 0.01	0.0037		
Ru/AC@PDA-800	Ru-O/N	6.5 ± 0.3	2.04 ± 0.01	0.0040	3.6 ± 1.2	0.0037

2 ^aN: coordination numbers; ^bR: bond distance; ^c σ^2 : Debye-Waller factors; ^d ΔE_0 : the inner potential3 correction. R factor: goodness of fit. S_0^2 was set to 0.71, according to the experimental EXAFS fit

4 of Ru foil reference by fixing CN as the known crystallographic value; δ: percentage.

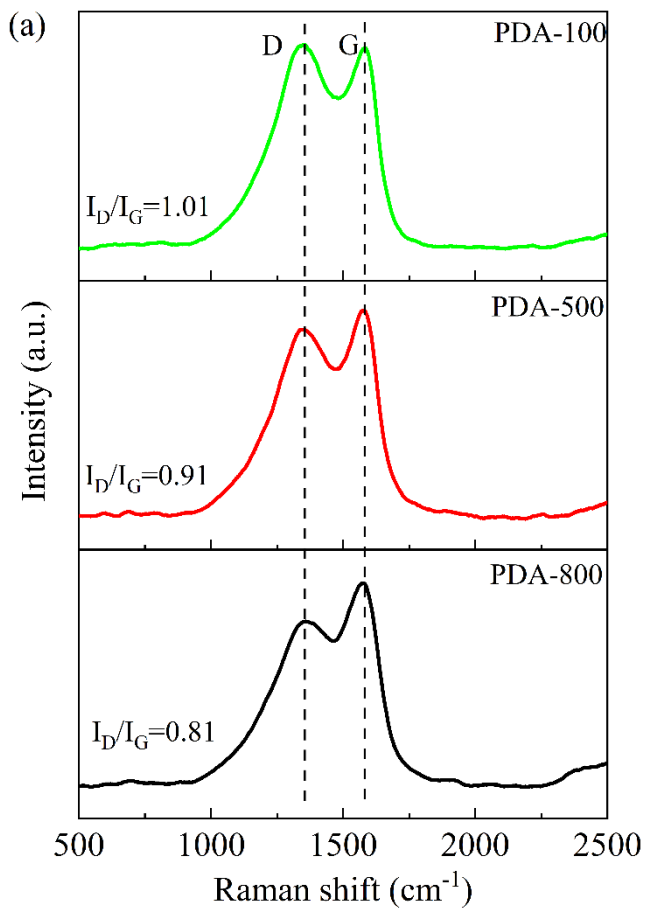
1



2

3 **Fig. S1** The (a) C_2H_2 conversion and (b) selectivity to VCM of different catalysts.4 Reaction condition: $T=180^\circ\text{C}$, $\text{GHSV}(\text{C}_2\text{H}_2)=180 \text{ h}^{-1}$, and $V(\text{HCl})/V(\text{C}_2\text{H}_2)=1.15$.

1



2

3

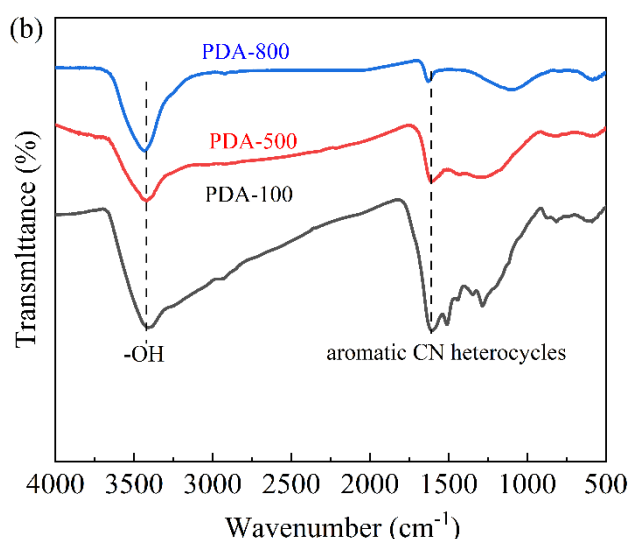


Fig. S2 (a) Raman spectra and (b) FT-IR spectra of PDA- T materials.

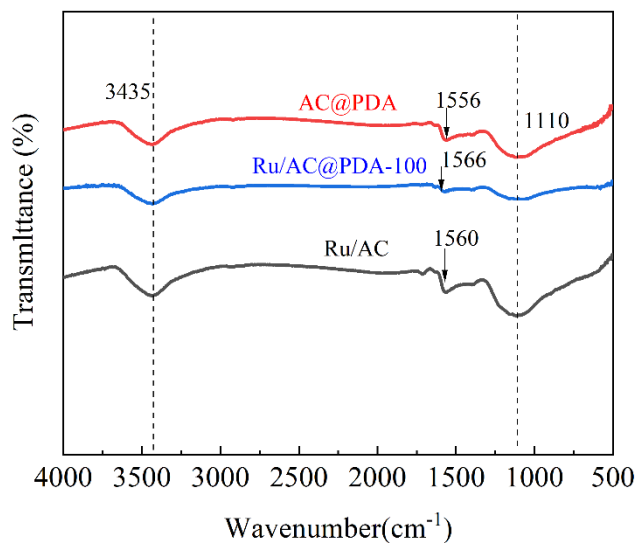
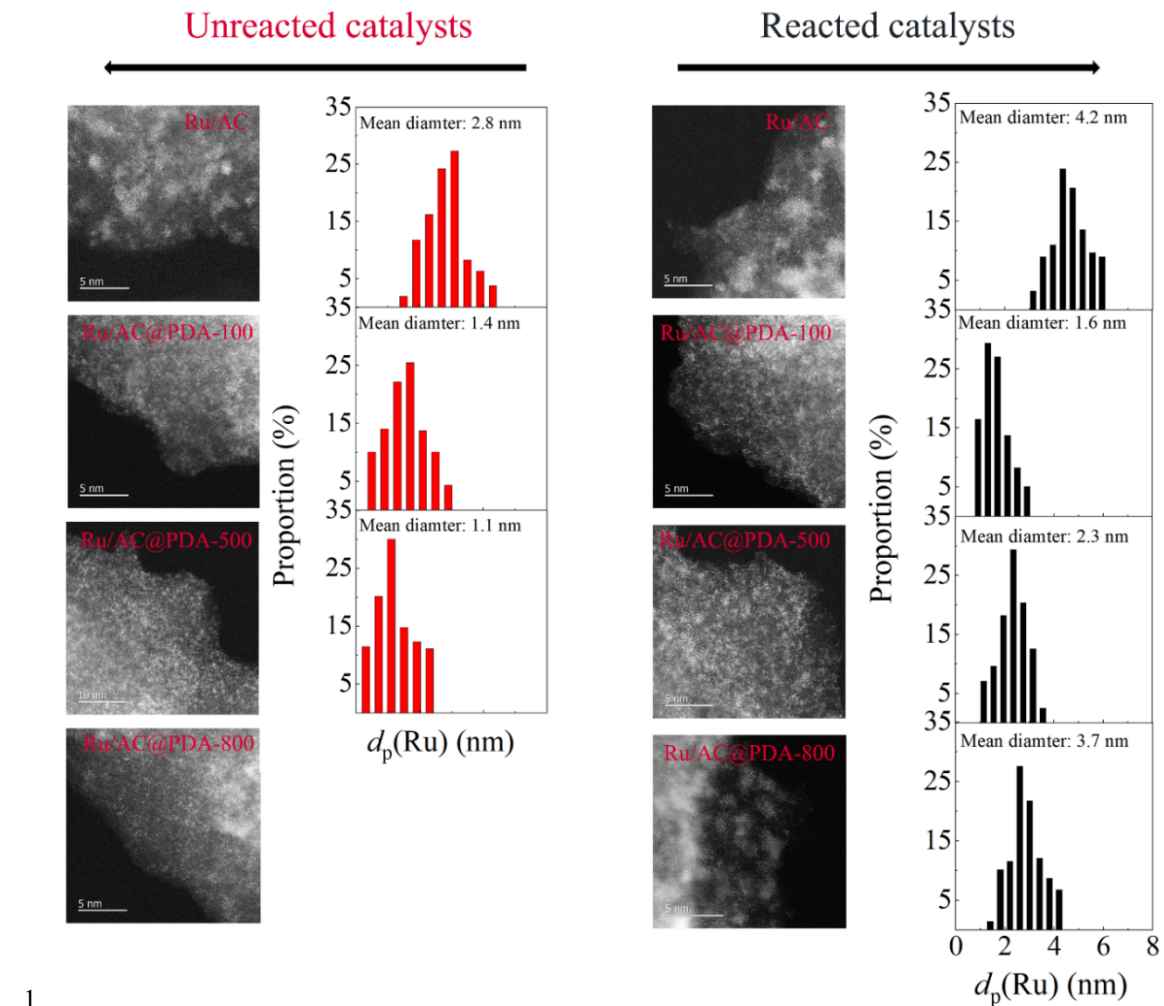


Fig. S3 FT-IR spectra of unreacted catalysts.

The characteristic peaks are centered at 3435 cm^{-1} : the -OH stretching vibration (e.g., those in phenol, carboxyl and chemisorbed water)¹, 1110 cm^{-1} : C-O stretching vibrations (e.g., ethers and phenols)^{2,3}, and 1560 cm^{-1} : aromatic CN heterocycles^{4,5}.



1

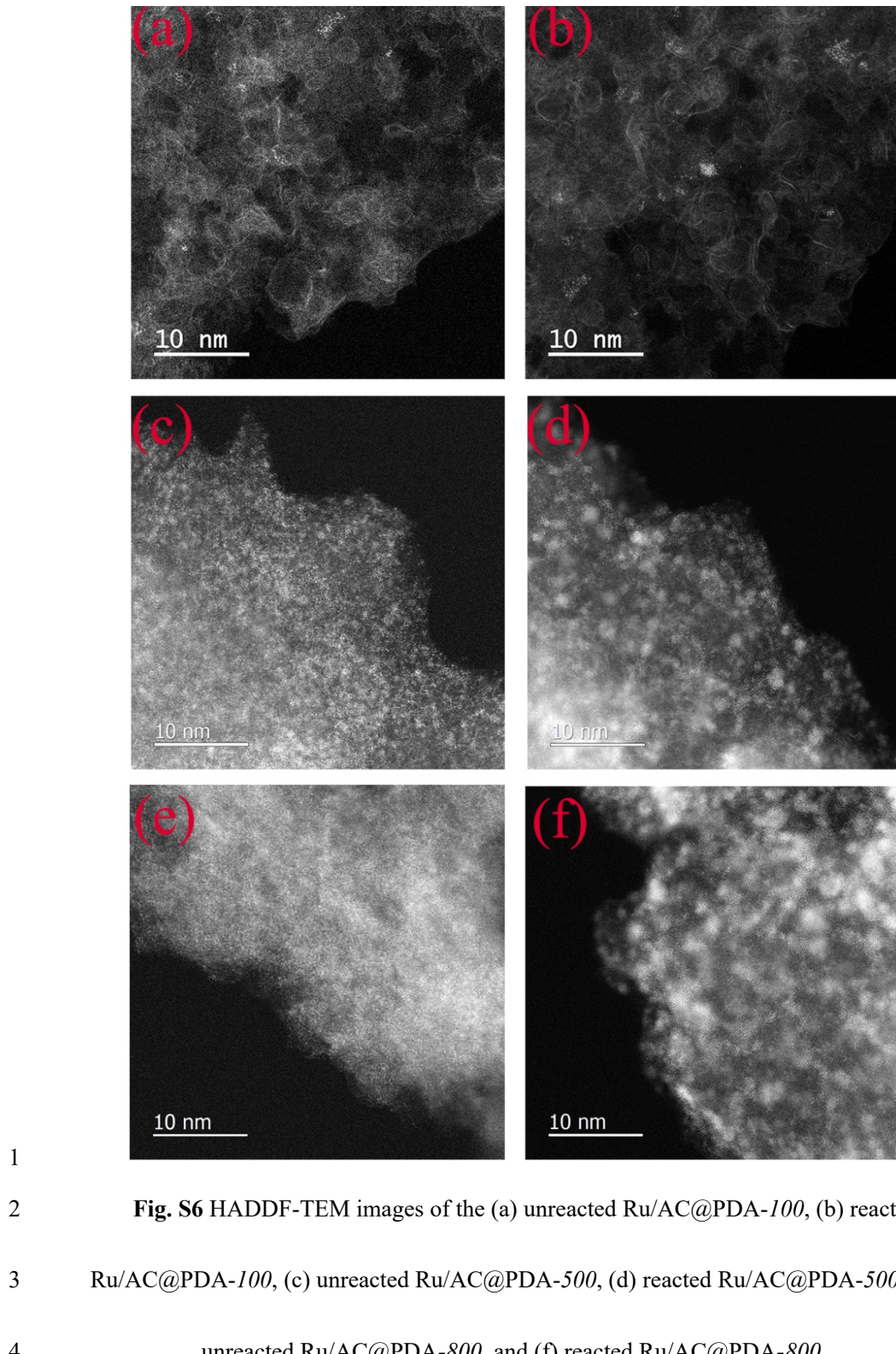
Fig. S4 HAADF-STEM images of the all catalysts.

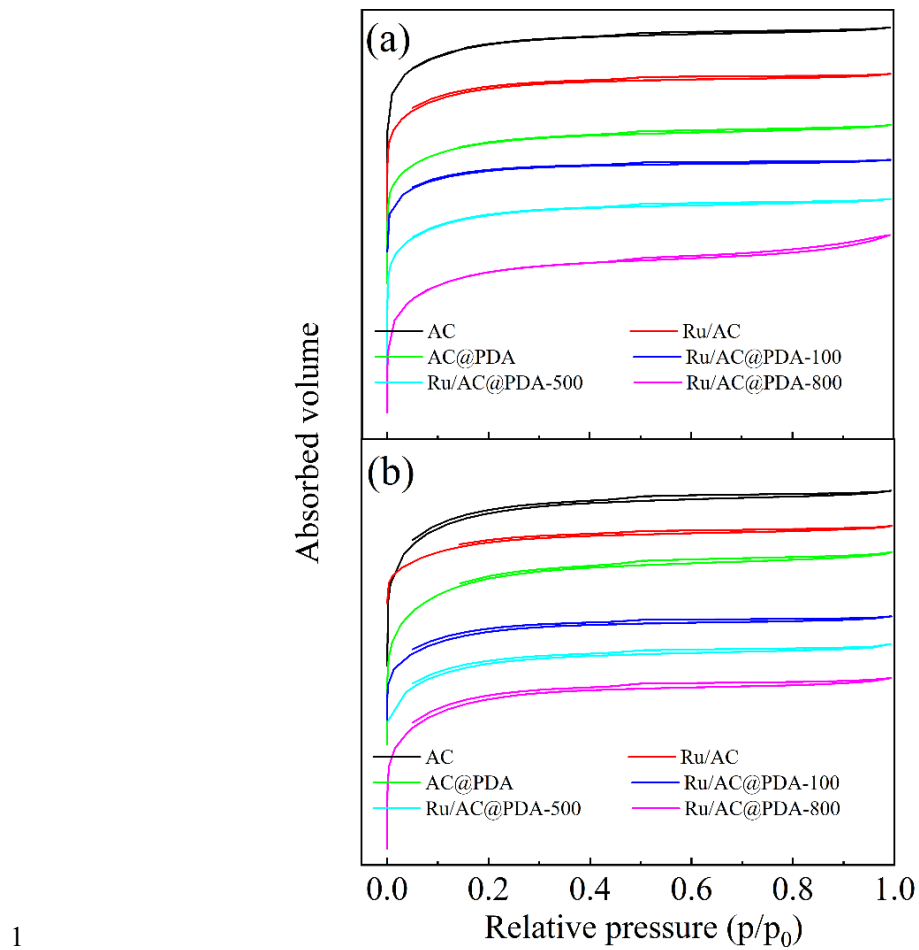
2 Synthesis of activated carbon (AC) supported ruthenium catalysts with varying ruthenium
 3 particle size (d_p (Ru)) via thermal activation at different temperatures, indicated in the sample
 4 code. HAADF-STEM images, with the respective metal particle size distribution, obtained from
 5 analysis of >150 particles, visualize a steady metal particle growth with an increasing activation
 6 temperature on carbon carriers.
 7

1

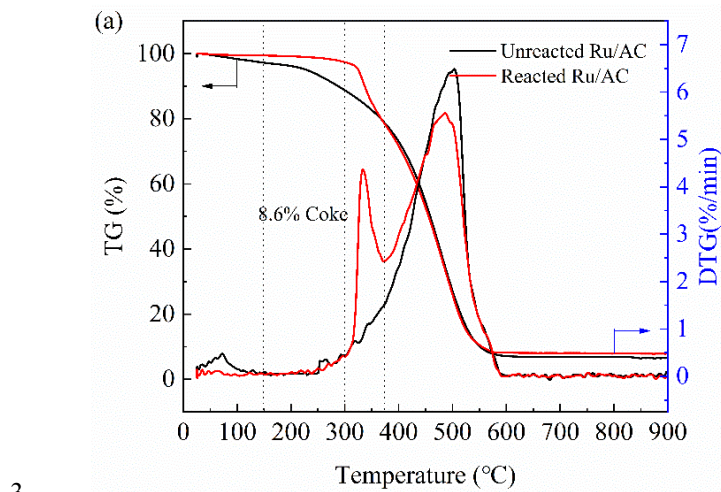


2 **Fig. S5** SEM images of the unreacted PDA catalysts.

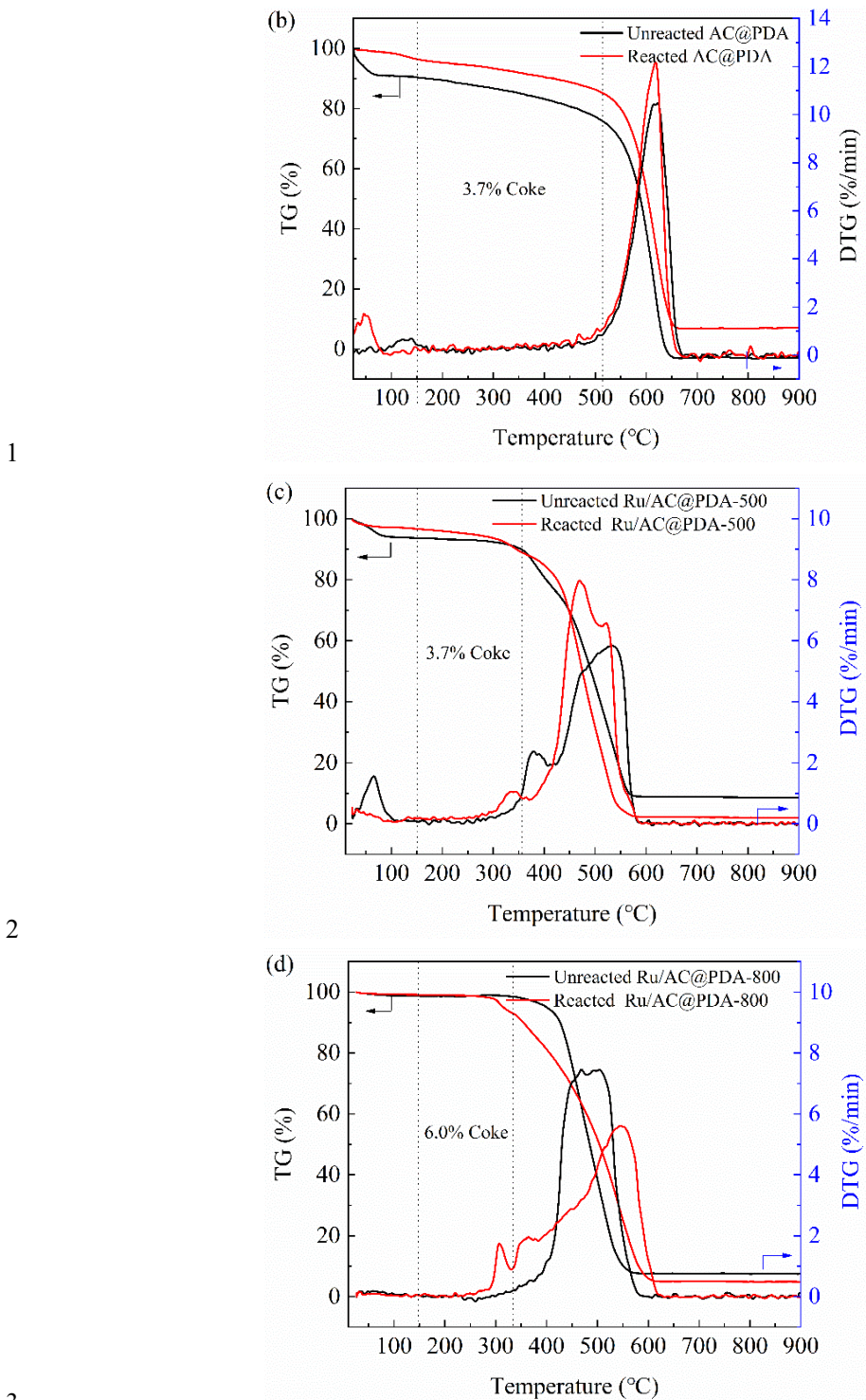




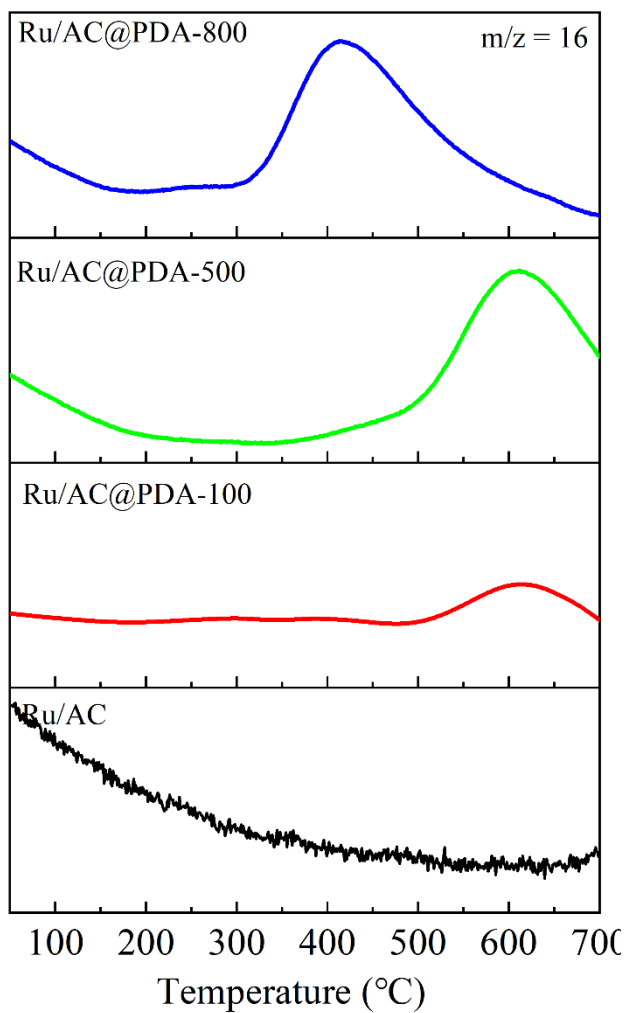
2 **Fig. S7** Nitrogen adsorption-desorption isotherms of the(a) unreacted and (b) reacted catalysts.



3

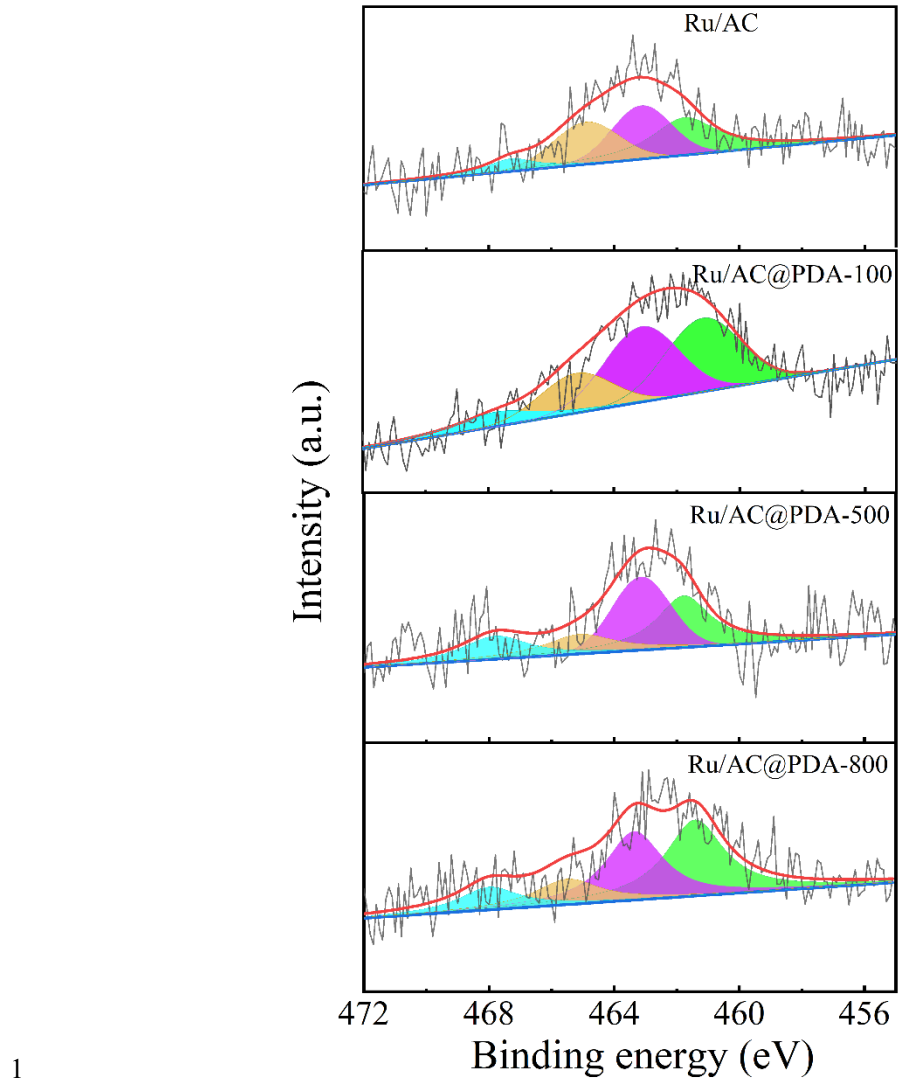


4 **Fig. S8** TG curves of the unreacted and reacted catalysts recorded under air atmosphere.



1
2

Fig. S9 MS spectra ($m/z = 16$) of the unreacted Ru catalysts.

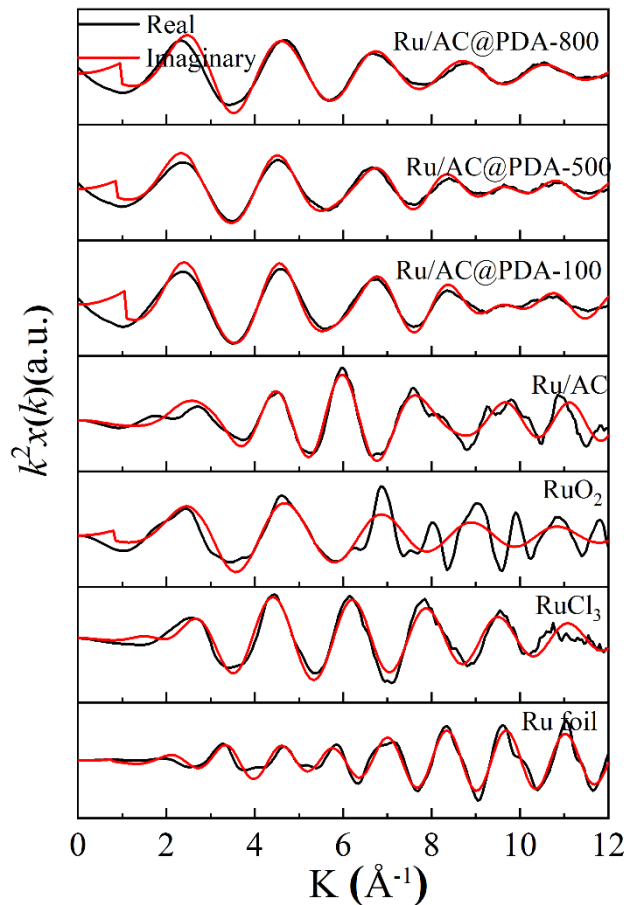


1

2

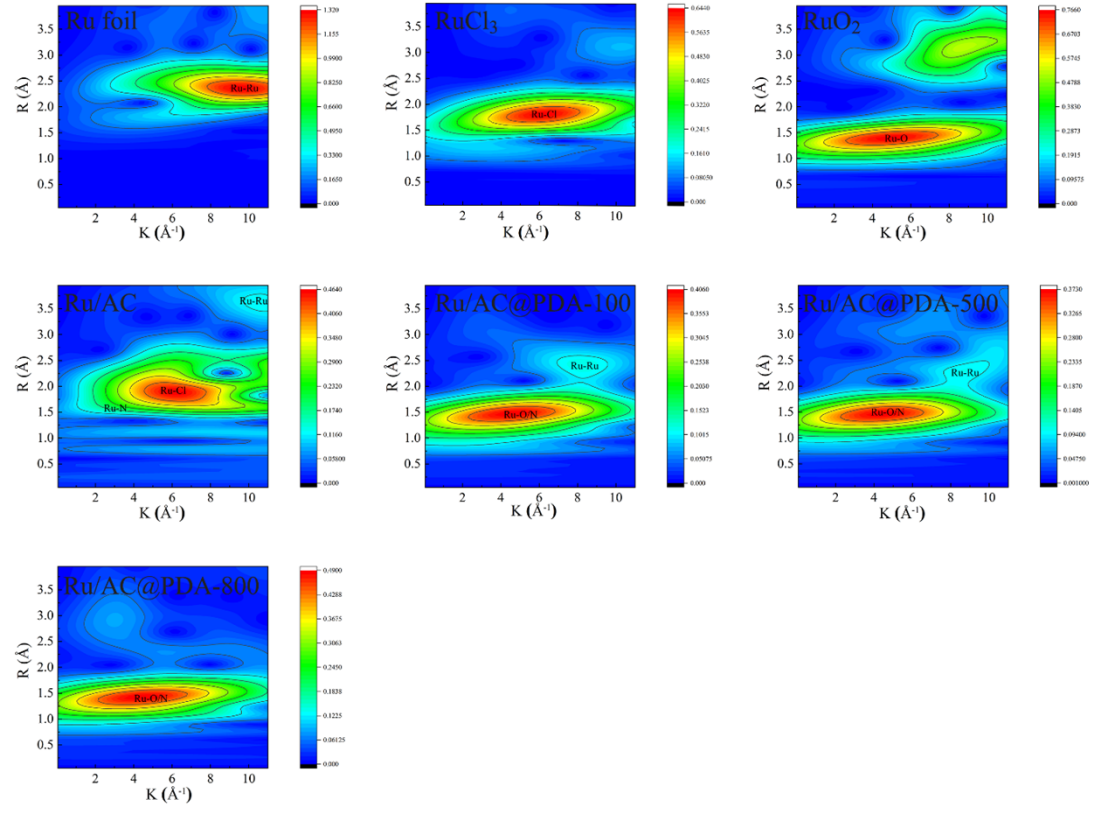
Fig. S10 Ru 3p XPS spectra of the reacted Ru catalysts.

1



2

3 **Fig. S11** The real/imaginary component of the FT with the scattering paths used in the fitting
4 models.



2

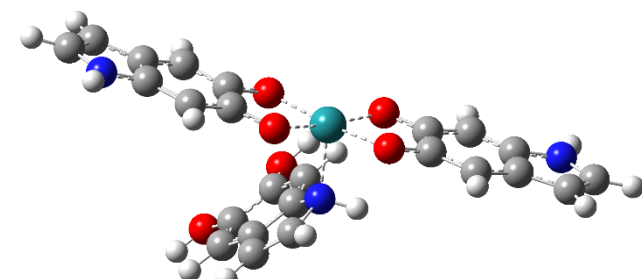
Fig. S12 Wavelet transform spectra of the Ru-based catalysts.

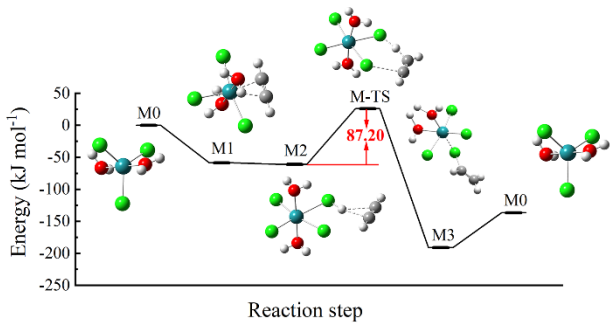
3

4 **Fig. S13** (a) N 1s XPS spectrum of the unreacted AC@PDA catalyst and (b) possible structure of
5 PDA.^{6,7}

6

7

**Fig. S14** The most stable calculation model of the complex.



1

2

Fig. S15 Energy profiles of Ru/AC catalyst for acetylene hydrochlorination.

1 References

- 2 1 A. M. Puziy, O. I. Poddubnaya, A. Martínez-Alonso, F. Suárez-García and J. M. D.
3 Tascon, *Carbon*, 2002, **40**, 1493-1505.
- 4 2 Y. Li, Q. Du, T. Liu, X. Peng, J. Wang, J. Sun, Y. Wang, S. Wu, Z. Wang, Y. Xia
5 and L. Xia, *Chem. Eng. Res. Des.*, 2013, **91**, 361-368.
- 6 3 A.-N. A. El-Hendawy, *Carbon*, 2003, **41**, 713-722.
- 7 4 Z. Shen, Y. Liu, Y. Han, Y. Qin, J. Li, P. Xing and B. Jiang, *RSC Adv.*, 2020, **10**,
8 14556-14569.
- 9 5 H. Zhang, Y. Wang, D. Wang, Y. Li, X. Liu, P. Liu, H. Yang, T. An, Z. Tang and
10 H. Zhao, *Small*, 2014, **10**, 3371-3378.
- 11 6 X. Li, P. Li, X. Pan, H. Ma and X. Bao, *Appl. Catal. B-Environ.*, 2017, **210**, 116-
12 120.
- 13 7 H. Lee, S. M. Dellatore, W. M. Miller and P. B. Messersmith, *Science*, 2007, **318**,
14 426-430.
- 15